Combined Static and Dynamic Light Scattering Study of Associating Random Block Copolymers in Solution

R. Klucker, J. P. Munch, and F. Schosseler*

Laboratoire d'Ultrasons et de Dynamique des Fluides Complexes, URA 851 Université Louis Pasteur, 4 rue Blaise Pascal, 67070 Strasbourg Cedex, France

Received November 19, 1996; Revised Manuscript Received April 10, 1997[⊗]

ABSTRACT: We combine static and dynamic light scattering techniques to study the structure and dynamics of hydrophobically modified polyacrylamide in aqueous solution. Two different length scales can be distinguished in the solutions. The first one corresponds to the usual structure of an ideal semidilute polymer solution, with a correlation length given by the size of the blobs. On that length scale, fluctuations of concentration relax by a cooperative diffusion mechanism. On a much larger length scale (>2000 Å), there is experimental evidence for a texture. The corresponding relaxation times appear to be related to the macroscopic viscosity of the surrounding polymer solution and might correspond to a viscoelastic relaxation of the texture embedded in this solution. This texture appears to be responsible for the interesting thickening properties of these associating random block copolymers.

I. Introduction

This paper is part of a series dealing with the properties of hydrophobically modified polyacrylamide in aqueous solutions. Previous papers have described the synthesis of these polymers[1−3] obtained through the radical copolymerization in micellar solution[4] of acrylamide and a small amount (∼1% mol/mol) of *N*-(4-ethylphenyl)acrylamide, a hydrophobic unit. The shear rate dependence of the steady-state viscosity of these samples in semidilute solution has been studied in pure water[1] as well as in the presence of added surfactant.[2] Due to the association of the hydrophobic units in aqueous solutions they show interesting thickening properties with an enhancement of the zero shear viscosity by a factor of about 10−20 relative to equivalent solutions of unmodified polyacrylamide with the same molecular weight.[3] Thixotropic effects were observed in these solutions, and the final value of the zero shear viscosity, measured after a succession of shear rate steps with increasing and then decreasing shear rate amplitude, was found to be smaller than its initial value. This result shows that the transient associative network is easily disrupted by the flow and needs typically several hours to rebuild in these systems.[3] More recently, the transient behavior of the solutions in a shear flow has been investigated.[5] The analysis of the results showed this transient rheological behavior is consistent with the transient associating network being depicted as a loosely connected network. Thus a large fraction of the chains are likely to be associated in free clusters, i.e. not connected to the largest percolating cluster, with a distribution of sizes that depends on the shear history. In a recent paper,[6] in an attempt to characterize the structure of these solutions at a microscopic level, we have compared the structure factors of polyacrylamide and hydrophobically modified polyacrylamide solutions measured by small angle neutron and X-ray scattering techniques on length scales up to about 200 Å. It has been shown that they are very similar up to length scales that correspond approximately to the correlation length ξ[7] of the semidilute solution, which was in the range 50−100 Å for the investigated polymer concentration $C = 0.03$ g/cm^3. Only at larger length scales was it possible to detect a slight increase in the fluctuations of polymer concentration in the copolymer solution compared to the homopolymer solution.

Therefore, in order to obtain more information on that effect on larger length scales, we performed static and dynamic light scattering experiments on homopolymer and copolymer solutions with varying polymer concentrations. The features most readily apparent in the first experiments were the strong angular dependence of the scattering intensity and the presence of fast and slow relaxation processes in its time autocorrelation function. Slow relaxation of concentration fluctuations have been reported for a wide variety of polymer systems in the past,[8−14] and several theoretical models have been proposed to explain these modes.[15−19] In order to distinguish their physical origin, it is necessary to determine how they contribute to the scattering intensity and whether their characteristic time is linked to an intrinsic characteristic time of the system (structure relaxation) or to a characteristic length probed in the measurement (diffusive process). For this purpose, the scattering wavevector dependencies for the scattering intensity and for the amplitudes and characteristic times associated with the relaxation modes must be carefully characterized. This can be done by a combination of the static and dynamic scattering techniques, which provides a powerful tool to better understand the physical mechanisms that are at the origin of the interesting rheological behavior of these systems. After giving the details of the experimental procedures and of the data analysis in section II, we describe the experimental results in section III and discuss them at length in section IV, in relation to a few selected models relevant to the experimental findings.

II. Experimental Part

1. Sample Preparation. Sample synthesis has been described in detail in other papers.[1−3] We just recall here that the samples are synthesized through radical copolymerization of acrylamide and *N*-(4-ethylphenyl)acrylamide in the presence of sodium dodecyl sulfate (SDS) micelles that solubilize the hydrophobic monomers. Reaction is initiated by sodium persulfate at 50 °C and is stopped by adding methanol hydroquinone at about 10% monomer conversion in order to avoid a large heterogeneity in the composition of the resulting copolymers.[2] The polymers are then precipitated in methanol

[⊗] Abstract published in *Advance ACS Abstracts,* June 1, 1997.

S0024-9297(96)01710-X CCC: $14.00

Table 1. Characteristics of the Samples

	polymerization parameters		polymer characterization		
sample	[SDS][a]	hydrophobe conc[b]	conversion[c]	hydrophobe content (mol %)	$10^{-6}M_w$
D	3	0	25	0	1.7
N	0	0	24.5	0	4.9
J	3	0.75	13	1.14	4.0

[a] SDS weight % in the feed, based on volume of water. [b] mol % in the feed, based on monomer concentrations. [c] weight %, based on initial monomer amount.

and washed repeatedly in methanol to remove the surfactant and unreacted monomers. After careful drying, the samples are kept in tightly closed containers in the dark until further use.

The hydrophobe content of the chains is measured by routine UV spectroscopy and their weight-averaged molecular weight by standard light scattering from dilute solutions in formamide, where no associating behavior is present. Table 1 summarizes the characteristics of the samples used in this study.

Solutions for the light scattering experiments are prepared with filtrated deionized water. The polymer is first allowed to hydrate and swell in water for 1 day. Then it is gently stirred for another day, and finally, it is allowed to rest for the next 2 days. The solution is then poured in the scattering cells, which are 13 mm glass tubes closed with a screwed cap. Thus they can be kept for months without evaporation or contamination taking place.

2. Light Scattering Setup. Experiments were performed with a thermoregulated home-built goniometer, equipped with an argon laser source operating at $\lambda = 4880$ Å. In these experiments the scattering angle θ has been varied between 20° and 130°, which corresponds to scattering wavevectors q in the range 6×10^{-4} to 3×10^{-3} Å^{-1}. A computer-driven stepping motor allows one to translate vertically the sample and to probe different scattering volumes. The scattering intensity $I(q,t)$ is measured by a photomultiplier through a set of two pinholes with diameters of 100 μm and 1.1 mm. The photocurrent is then processed by a photon counting device for static light scattering measurements or by an ALV 5000 correlator for dynamic light scattering measurements. The latter device computes the normalized time correlation function of the scattering intensity, $g^{(2)}(q,t) = \langle I(q,0)\, I(q,t)\rangle/\langle I(q,t)\rangle^2$, for pseudologarithmically spaced delay times t in the range 0.4 μs to 430 s when it is used in dual mode. The electric field autocorrelation function $g^{(1)}(q,t) = \langle E(q,0)\, E^*(q,t)\rangle/\langle I(q,t)\rangle$ can be calculated from $g^{(2)}(t)$ through Siegert's relationship:[20]

$$g^{(2)}(q,t) = 1 + \beta^2 |g^{(1)}(q,t)|^2 \qquad (1)$$

where the coherence factor β is determined by the geometry of the detection. In our case β is about 0.9, as determined by measuring the amplitude of the correlation function for a dilute solution of latices. Calibration of the static scattering intensity values is obtained by using the intensity scattered from pure toluene as a standard.

3. Experimental Procedures. The samples investigated in this study are characterized by large intensity fluctuations with long relaxation times (up to tens of seconds) and have required special procedures of measurements in order to obtain sensible and reproducible results.

As an example, Figure 1 displays the static structure factor $I(q) \equiv \langle I(q,t)\rangle$ of a copolymer solution with polymer concentration $C = 0.03$ g/cm^3, obtained with a standard method where each data point corresponds to an average intensity measured over a few milliseconds. Clearly, this time is not long enough to measure a good average value and the results are very noisy (open symbols). The true average value can be obtained by translating the samples and by probing a large number (400) of different scattering volumes, following the procedures designed for the study of swollen gels.[21−23] This method provides a smooth curve (closed symbols in Figure 1) that corresponds to intensity values averaged over a large enough

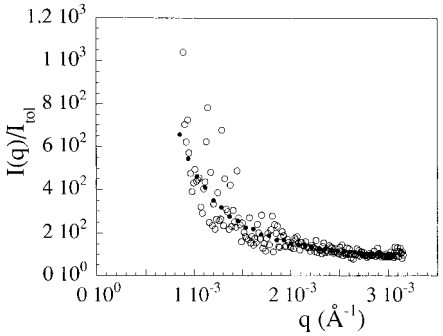

Figure 1. Light scattering intensity measured as a function of scattering wavevector for a copolymer sample at $C = 0.03$ g/cm^3. Open circles correspond to intensity values averaged over a few milliseconds, while closed circles indicate average values calculated from measurements performed on 400 different scattering volumes, as explained in the text.

set of configurations for the system. In principle, the same result could have been obtained by enlarging the size of the pinholes in the experimental setup in order to increase the scattering volume. However, the latter method is more difficult to use in practice because it increases the risk of measuring stray light due to reflections of the incident beam in the apparatus.

Special care must also be paid to obtain meaningful correlation functions for these systems. In particular, very long measurement times (up to 10 h) can be necessary to obtain both the full amplitude $1 + \beta^2$ of the intensity−intensity correlation function and a good asymptotical value at large times (typically 1 ± 0.001). In order to test reproducibility, we required three measurements with these criteria fulfilled for each scattering angle.

4. Data Analysis. The intensity correlation functions of homopolymer and copolymer solutions with polymer concentration between 10^{-3} and 3×10^{-2} g/cm^3 are characterized by two distinct relaxation processes with amplitudes and rates of relaxation that depend strongly on scattering angle and polymer concentration.

The data have been analyzed with the help of the CONTIN program[24] implemented on a desktop computer. In the first step, CONTIN parameters were set to fit the $g^{(2)}(t)$ functions as

$$g^{(2)}(t) = \sum_{i=1}^{40} p'(\tau_i) \exp(-t/\tau_i) + g_\infty \qquad (2)$$

where the $\{p'(\tau_i), \tau_i\}$ are positive fitting parameters and g_∞ defines the asymptotical value of $g^{(2)}(t)$. In the second step, $\beta g^{(1)}(t)$ was calculated as $[g^{(2)}(t) - g_\infty]^{1/2}$ and the CONTIN program was run with the values of $\beta g^{(1)}(t)$ that remain above twice the root mean square (rms) deviation around the asymptotical zero value. This criterion was found quite effective in preventing unphysical relaxation times from appearing in the analysis due to the experimental noise. In this second step, CONTIN parameters were set to fit $\beta g^{(1)}(t)$ as

$$\beta g^{(1)}(t) = \sum_{i=1}^{40} p(\tau_i) \exp(-t/\tau_i) \qquad (3)$$

i.e., with g_∞ set to zero.

It can be noted that the definition of $p'(\tau_i)$ in the first step (eq 2) gives this function no real physical meaning and only allows us to determine g_∞ in a way consistent with the CONTIN analysis. An alternative procedure could have been to get g_∞ from the average value of $g^{(2)}(t)$ in the last channel and then to proceed through the second step. However, in practice, this is not very accurate for systems with very long relaxation times. On the other hand, CONTIN would allow a direct fit of $[g^{(2)}(t) - 1]^{1/2}$ with an additional floating base line but this would likely introduce artefacts related to the

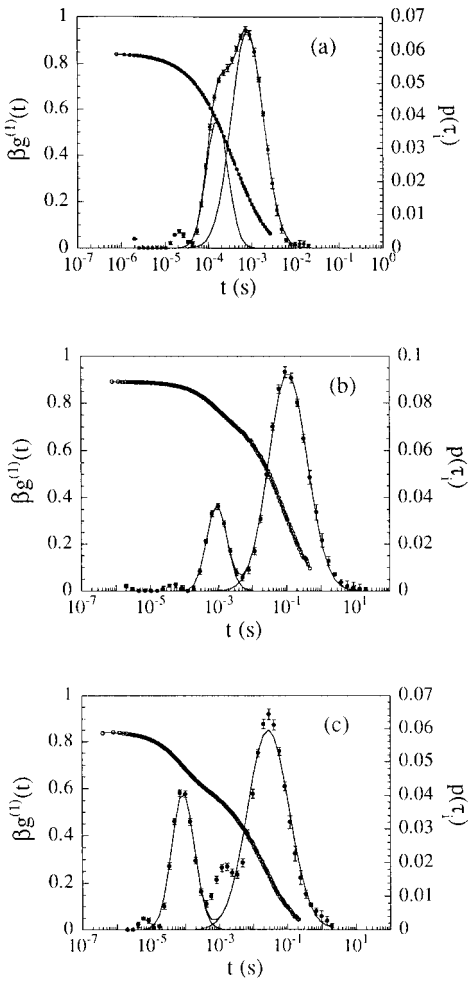

Figure 2. Typical examples of CONTIN analysis of the field autocorrelation function $\beta g^{(1)}(t)$ for copolymer sample J at different concentrations and scattering angles: (a) $C = 10^{-3}$ g/cm^3, $\theta = 110°$; (b) $C = 5 \times 10^{-3}$ g/cm^3, $\theta = 40°$; (c) $C = 10^{-2}$ g/cm^3, $\theta = 120°$. Each plot displays the correlation function as opened circles, the continuous line through them being the CONTIN fit, and the corresponding distribution of relaxation times (closed circles) with error bars on the $p(\tau_i)$ as calculated by the program. The distribution is fitted by the sum of two log-normal curves that are shown as well as their sum as continuous lines.

experimental noise: in fact CONTIN deals with fluctuations of the variable A around a zero value by defining $A^{1/2} \equiv \mathrm{sgn}(A)|A|^{1/2}$, where sgn($A$) is the sign function, and this definition can easily produce artefacts when the base line is defined by only a few channels. Thus, although our two-step analysis appears complicated and time consuming, it produces more dependable results.

Unphysical relaxation times can also appear if an inappropriate window of relaxation times is provided to the program: in this case, the unphysical components are used to describe better the experimental noise. In our case, the lower limit of the time window was set to 2 μs and the upper limit was given about 10 times the delay time in the last channels used in the analysis of $\beta g^{(1)}(t)$.

Typical examples of electric field correlation functions together with their CONTIN analysis are shown in Figure 2. As a first comment, it appears clearly that the CONTIN program is in general very successful in producing a smooth function that follows very nicely the experimental correlation functions. Thus the agreement between the calculated and the experimental correlation functions is by no means a sufficient criterion for the quality of the fit. The latter can only be estimated from the behavior of the $p(\tau_i)$ curve. We can note first that CONTIN is providing error bars for the $p(\tau_i)$, which can help in rejecting some results. An additional hint

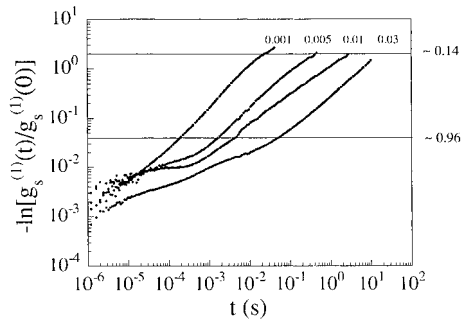

Figure 3. Plot on logarithmic scales of the natural logarithm of the normalized slowly decaying part in the field autocorrelation function (see text). In such a plot, a stretched exponential decay appears as a straight line. Horizontal lines denote the levels corresponding to $g_s^{(1)}(t)/g_s^{(1)}(0) \simeq 0.96$ and $g_s^{(1)}(t)/g_s^{(1)}(0) \simeq 0.14$. Other numbers indicate the polymer concentration of copolymer J solutions ($\theta = 40°$).

can be obtained by comparing the results from different measurements at the same scattering angle and concentration. In general, they are reproducible, with the amplitudes being less robust than the characteristic times. The overall shape of the $p(\tau_i)$, is also most often rather well established, with the wings being more sensitive to the upper and lower limits of the time window. For the two smallest polymer concentrations (Figures 2a,b), it appears generally as two peaks that merge more or less according to the scattering angle and the polymer concentration. For the highest polymer concentrations investigated here ($C = 0.01$ and 0.03 g/cm^3), however, this feature is less clear as a third maximum is appearing between the two largest peaks (Figure 2c).

Interestingly, we find that for the smallest concentrations, the $p(\tau_i)$ curve can be successfully described by the sum of two log-normal curves (Figure 2a,b). For the highest concentrations, while the short-times part can still be fitted by a log-normal curve, it is no longer the case for the behavior at long times (Figure 2c). This functional dependence might well be related to the particular sampling of delay times built in the correlator. On the other hand, it can be used for the deconvolution of the fast and slow relaxation times, as shown in Figure 2.

Then average values for the characteristic times of the fast and slow relaxation modes can be calculated. It turns out that the q dependence of the slow relaxation times obtained in this way can be described by a power law with an exponent around -3. This suggests a different analysis of the slow relaxation process as a stretched exponential. Although this analytical form of the correlation function can be justified theoretically in some cases,[8,25−28] it is here only a convenient method to define an average relaxation time consistently in the whole concentration range. Therefore, in a third step, we subtracted from the experimental $g^{(1)}(t)$ the fast relaxation as described by the $p(\tau_i)$ obtained through the CONTIN analysis. The remaining part $g_s^{(1)}(t)$ was then fitted by a stretched exponential as

$$g_s^{(1)}(t) = A_\alpha \exp[-(t/\tau_\alpha)^\alpha] \qquad (4)$$

The possibility of subtracting the contribution of one relaxation mode to a multimode correlation function arises naturally from a principle of linear superposition and has been proposed before,[29] although in a slightly different spirit. Here the subtraction of the minor fast contribution only allows us to fit more conveniently the remaining part of the function and to plot it in the representation appropriate for the stretched exponential decay. Figure 3 shows that typical $g_s^{(1)}(t)$ can be described satisfactorily by a stretched exponential behavior for times larger than some characteristic cutoff τ_o. Usually, this behavior extends over two decades in time.

We have now to make a somewhat arbitrary choice to define average times. In the case of the fast relaxation, the most usual definition would use the slope of the correlation function at the origin, i.e. the average $\langle \tau^{-1} \rangle$ of $1/\tau$ over the distribution

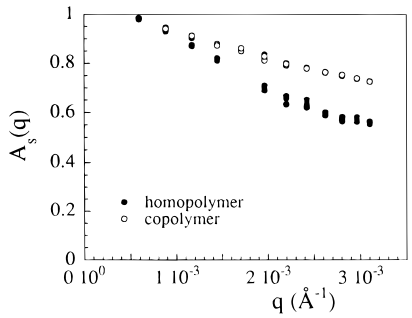

Figure 4. Scattering wavevector dependence of the amplitude of the slow mode in homopolymer and copolymer solutions with $C = 10^{-2}$ g/cm^3.

of relaxation times. Such a definition makes no sense for the slow relaxation if it is described by a stretched exponential, where the short time behavior is not defined below the cutoff τ_o. In that case a characteristic time τ_s with a physical meaning is given by the integral of the stretched exponential:

$$\tau_s = \int_{\tau_o}^{+\infty} \exp[-(t/\tau_\alpha)^\alpha]\, dt \simeq \Gamma(1/\alpha)\, \tau_\alpha/\alpha \qquad (5)$$

where $\Gamma(x)$ is Euler's gamma function.

If we compare that value to the results obtained with the CONTIN method, we find that it lies in between $\langle\tau^{-1}\rangle^{-1}$ and $\langle\tau\rangle$ and that it is pretty much the same as the value at the peak of the distribution when the latter can be fitted by a log-normal curve. Therefore, to be consistent in the definition of fast and slow relaxation times, we choose to use the position of the peak as a measure of the fast characteristic time τ_f. We checked that our results are not altered significantly by our particular choices for τ_f and τ_s and in particular that their q dependence remained the same. Moreover, we found that the definitions here adopted yield a significant reduction of scattering in the data.

The amplitudes of the two relaxation processes have been defined as

$$A_f \equiv \frac{1}{\beta}\sum_{\text{fast}} p(\tau_i) \qquad (6)$$

$$A_s \equiv 1 - A_f$$

where the β factor arises from the fact that in the second step of the analysis we applied the CONTIN program to $\beta g^{(1)}(t)$. It is worth noting that in fact these amplitudes are dependent on the scattering wavevector, as shown in Figure 4.

The amplitudes of the modes measured in the dynamic light scattering experiment can be used to analyze the static light scattering results.[14,30−32] Writing the scattered field as the sum of two electric fields $E_f(q,t)$ and $E_s(q,t)$ that are fluctuating independently, it is easy to show that[20]

$$g^{(1)}(q,t) = \frac{\langle E_f(q,t')\, E_f^*(q,t'+t)\rangle + \langle E_s(q,t')\, E_s^*(q,t'+t)\rangle}{I(q)} \qquad (7)$$

where the cross-correlation terms vanish due to the time average. Defining $I_f(q)$ and $I_s(q)$ as the time-averaged intensities associated with the fluctuations of polymer concentration with respectively short and long relaxation times and using the normalization condition $g^{(1)}(q,0) = A_f(q) + A_s(q) = 1$, we obtain

$$I_f(q) = A_f(q)\, I(q)$$
$$I_s(q) = A_s(q)\, I(q) \qquad (8)$$

Figure 5 shows such an analysis for a copolymer solution with $C = 5 \times 10^{-3}$ g/cm^3.

III. Results

1. Fast Relaxation Mode. In both homopolymer and copolymer solutions, the fast relaxation mode is

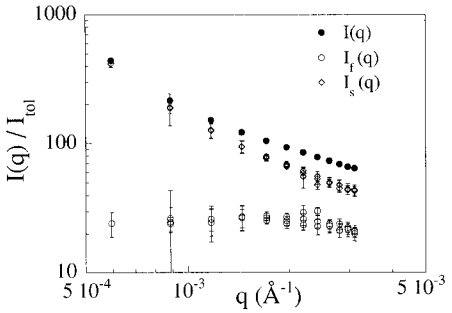

Figure 5. Decomposition of the total scattering intensity into the contributions associated with the fast and slow decay modes in the field autocorrelation function (copolymer J, $C = 5 \times 10^{-3}$ g/cm^3).

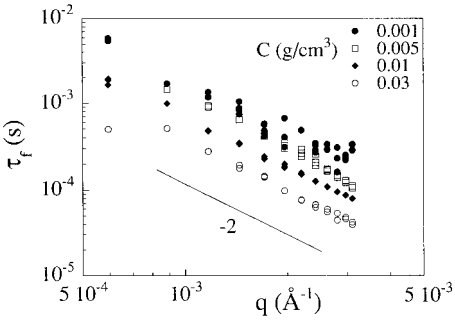

Figure 6. Variation with scattering wavevector of the fast characteristic times measured in copolymer J solutions with different concentrations.

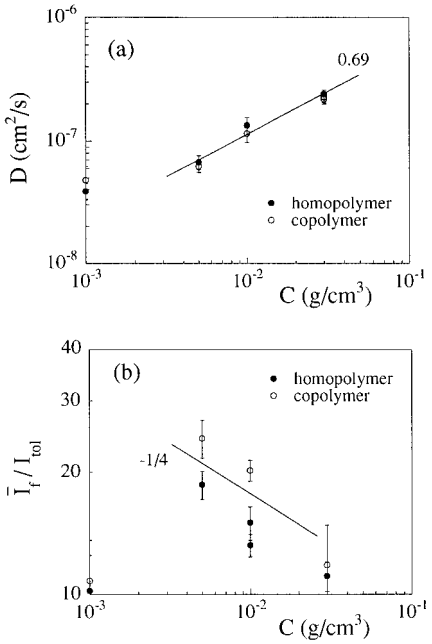

Figure 7. Dependence on polymer concentration of the diffusion coefficient (a) and of the average scattering intensity (b) associated with the fast decay mode. In (a) the line corresponds to a fit, while in (b) it only displays the expected slope for a semidilute solution in a good solvent.[6]

associated with a diffusive-like behavior, i.e. $\tau_f \sim q^{-2}$, as shown in Figure 6, and the corresponding intensity is independent of the scattering wavevector q (Figure 5). Thus it is possible to calculate for each polymer concentration a diffusion coefficient D and an intensity $\bar{I}_f$ averaged over all q values. The variations of these quantities with polymer concentration, displayed in Figure 7, are typical for polymer solutions in the dilute and the semidilute regimes, the transition between these two regimes occurring for polymer concentrations

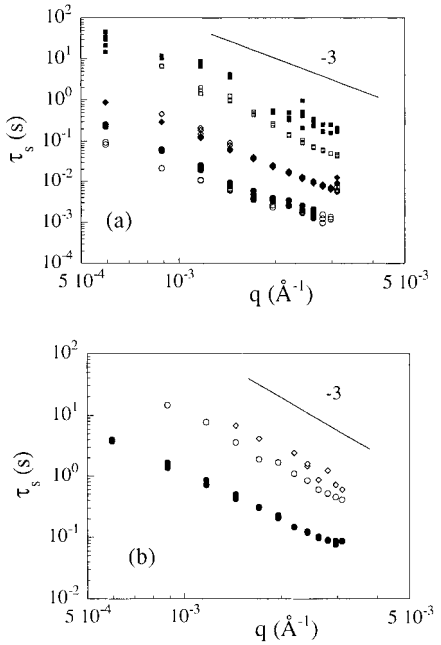

Figure 8. Variation with scattering wavevector of the slow characteristic times measured in homopolymer (closed symbols) and copolymer (opened symbols) solutions with different concentrations: (a) $C = 10^{-3}$ g/cm^3 (circles), $C = 5 \times 10^{-3}$ g/cm^3 (diamonds), $C = 10^{-2}$ g/cm^3 (squares); (b) $C = 3 \times 10^{-2}$ g/cm^3. At the (b) concentration, we used homopolymer D, compared to N for the lower ones in (a) (see text). For the copolymer data, diamonds and circles correspond to an aging time of 56 and 150 days, respectively.

Table 2. Values of the Exponents Characterizing the *q* Dependence of the Slow Relaxation Time[a]

C (g/cm^3)	homopolymer	copolymer
10^{-3}	3.4	2.6
5×10^{-3}	3.1	3.5
10^{-2}	3.2	4.0
3×10^{-2}	2.4	3.0

[a] For the highest concentration, the homopolymer sample is sample D, compared to N for the smaller concentrations. The copolymer sample is always sample J (see text).

between 0.001 and 0.005 g/cm^3. At high concentrations, the variations with polymer concentration are consistent with the behavior expected for a semidilute solution in a good solvent,[7] i.e. $\bar{I}_f \sim C^{-1/4}$ and $D \sim C^{3/4}$. An estimation for a correlation length ξ[7] from the D values at $C = 0.03$ g/cm^3 yields $\xi = 90$ Å. It can be emphasized that homopolymer and copolymer solutions can hardly be distinguished as far as the fast relaxation process is concerned. This is entirely consistent with our previous small angle neutron and X-ray scattering results[6] where we found that the fluctuations of overall polymer concentration were identical in both systems up to length scales of about 100 Å when $C = 0.03$ g/cm^3.

2. Slow Relaxation Mode. The slow relaxation times are characterized by a stronger q dependence (Figure 8) than found for the fast relaxation mode. This dependence can be described by a power law behavior with exponents ranging between -2.4 and -4 (see Table 2).

For the lowest polymer concentrations, these characteristic times are the same in the homopolymer and copolymer solutions within the experimental errors. For $C = 0.01$ g/cm^3, they are about 3 times larger in the homopolymer solution than in the copolymer solution. For the highest concentration (Figure 8b), this relation is inversed and the copolymer solution has characteristic slow times about 7 times larger than the corresponding homopolymer solution. However, one has to keep in mind that for the latter concentration, the homopolymer sample is sample D instead of sample N (see Table 1).

At that point, it is important to make the following remarks concerning the samples. When they are prepared along the lines described in the Experimental Part, we found that, except for the less concentrated solutions, it was not possible to measure immediately correlation functions that met the standards we required for the amplitude and for the base line of the correlation function. Instead, we had to wait a few weeks before good experiments could be performed. This improvement is due to a decrease with aging time of the characteristic times associated with the slow relaxation process. This effect is best seen in Figure 8b where are reported the τ_s values measured for copolymer J solution with $C = 0.03$ g/cm^3 about 56 days (diamonds) and 150 days (open circles) after sample preparation. The decrease in characteristic times is, in that particular case, by a factor slightly less than 2. Similarly, for the most diluted copolymer sample (Figure 8a), the measurements for the three smallest scattering angles have been performed after about 70 days instead of 40 days for the remaining ones and after 38−39 days for the whole q range in the homopolymer sample. For the sake of completeness, the aging time is 12−15 days for homopolymer and copolymer solutions with $C = 0.05$ g/cm^3, 60 days for copolymer solutions with $C = 0.01$ g/cm^3 (except for the two smallest scattering angles where it is 72 days). Finally homopolymer D at $C = 0.03$ g/cm^3 has been studied 250 days after preparation.

Aging effects have already been reported[5] for the rheological properties of these solutions. It was then noted that higher temperatures were speeding the observed decrease of the shear viscosity with aging time. We checked for such effects in dynamic light scattering with copolymer sample J at $C = 0.005$ g/cm^3 and for $\theta = 60°$. First it was verified that the correlation functions measured successively at $T = 291$ K, then at $T = 323$ K, and finally back at 291 K could be superposed by renormalizing the time scale with the proper factor $kT/\eta_o(T)$ where $\eta_o(T)$ is the temperature dependent viscosity of the solvent. These measurements were done 94 days after the preparation of the sample, which was then annealed for 24 h at $T = 323$ K and cooled to $T = 291$ K. A new measurement of the correlation function was done when the aging time was 101 days. Figure 9a shows the correlation functions measured at 291 K together with one that was measured in the initial series (aging time 15 days), and it is clear that aging is still taking place on these long time scales, resulting in a decrease of the slow relaxation time. CONTIN analysis shows that the amplitudes of the two relaxation processes are not altered by the aging and gives τ_s values about 2.77×10^{-2}, 1.91×10^{-2}, and 1.12×10^{-2} s (Figure 9b). The same test was done with homopolymer N at the same concentration and scattering angle, and the annealing was found to have no effect on the long relaxation time. At present, it is not possible to decide which mechanisms govern these aging effects. It was previously proposed that, in the case of copolymer samples with a large heterogeneity in composition, the decrease in viscosity was linked to a slow phase separation into regions containing highly modified chains and regions containing nearly pure homopolymer chains. For samples obtained at low conversion of the polymerization reaction, the heterogeneity in composition is re-

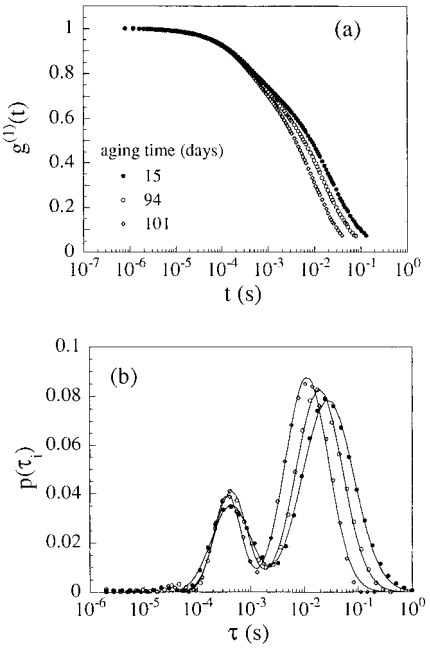

Figure 9. Effect of aging time on the dynamics of copolymer J solution with $C = 5 \times 10^{-3}$ g/cm^3 ($\theta = 60°$): (a) correlation functions; (b) corresponding CONTIN distributions. The continuous lines display the fit as a sum of two log-normal curves. See text for aging conditions.

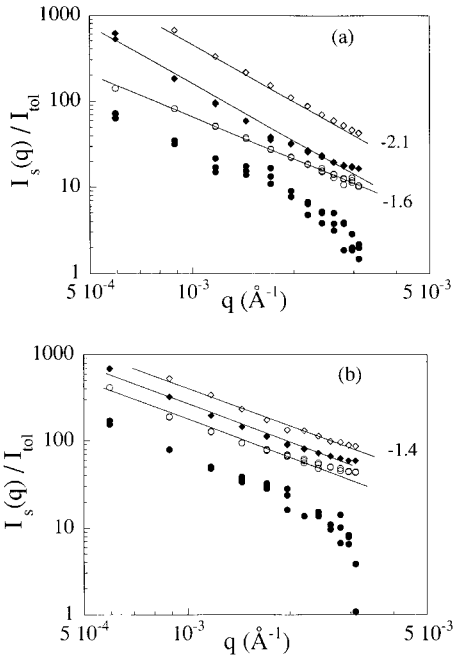

Figure 10. Scattering wavevector dependence of the scattering intensity associated with the slow component in homopolymer (a) and copolymer (b) solutions with different concentrations: from the bottom to top of each plot $C = 10^{-3}$, 5×10^{-3}, 10^{-2}, and 3×10^{-2} g/cm^3.

duced and this mechanism is less likely. In the Discussion, we will offer another explanation linked to the known aging phenomena in pure polyacrylamide solutions. It seems, however, that this aging corresponds to an evolution toward thermal equilibrium and that no degradation takes place. Thus this would mean that experiments performed a few days after the preparation of the samples, as in most rheology experiments and in most technological applications, probe some state of the solution that differs to some extent from the final thermodynamic equilibrium state, as often happens for systems with very slow dynamics.

Now back to the q dependence of the slow relaxation times, it is likely that the scattered exponent values in Table 2 may reflect partly the difficulty of measuring characteristic times in the range 0.1−50 s by dynamic light scattering techniques and partly the effects of different aging times. In fact a mean value of the exponent around −3 seems consistent with most of the data (Figure 8). Although aging effects are present, they are not large enough to blur the effects of polymer concentration except for the particular case of homopolymer D (Figure 8b), for which, however, other effects to be discussed later on can interfere. As a general trend, the characteristic time of the slow relaxation mode increases with polymer concentration.

The scattering intensity associated with the slow fluctuations of polymer concentration is also increasing with polymer concentration (Figure 10). At a given concentration the level of this scattering intensity is in general lower in the homopolymer solutions than in the copolymer solutions, but this difference is varying with scattering angle since the q dependence appears stronger in the former. Taking into account the experimental accuracy, this q dependence of I_s can be reasonably well fitted by a power law except for the smallest concentration. In this case, however, it is difficult to evaluate the significance of the downward curvature at large q values since these data have been obtained from CONTIN results where the separation of the two relaxations is not clear (Figure 2a). Values for the exponents of the forced power law are between −2.1 and −1.6 for the homopolymer solutions and about −1.4 for the copolymer solutions. One might be tempted to use sometimes two different exponent values to describe the behavior at small and large q values like, e.g., for the homopolymer sample at $C = 0.01$ g/cm^3 (Figure 10a). However, one has to keep in mind that the data in Figure 10 result from a complex analysis and that, moreover, light scattering data from aqueous systems with strong angular variation of the scattering intensity can be contaminated by stray light and multiple reflections of the scattered light due to the mismatch between the indices of refraction of the glass cell and of the solution. Therefore, emphasis should not be put on the power law behavior and the values of the exponents, but rather on the fact that no characteristic length can be obtained through the variation of $I_s(q)$ with scattering wavevector.

IV. Discussion

Slow relaxation of polymer concentration fluctuations is not an uncommon feature for polymer solutions in the semidilute or concentrated regimes and has been observed in a number of different systems including linear neutral polymers in good[9] or theta[10] solvent, branched polydisperse polymers in a good solvent,[8] polyelectrolyte solutions in the presence[11] or in the absence of added salt,[11,12] and associating polymer solutions.[13,14]

Although the generic name of slow mode relaxation is widely used, its physical origin may differ according to the system considered. In particular, dynamic coupling of elementary processes,[27,28] coupling of stress and polymer concentration fluctuations,[15−19] or diffusion of large particle aggregates[9,12] are possible mechanisms that might be responsible for a slow component in the decay of the intensity−intensity correlation function apart from a fast component that is in general more

easily understood. The variations of the relative amplitudes of the two modes, of the associated scattering intensities and rates of relaxation as a function of scattering wavevector and polymer concentration should in principle allow us to decide which mechanism is suitable for a given system. In the present case, however, it is not possible to point out a single mechanism that can consistently explain all the experimental facts.

The coupling model has been used by Nyström and co-workers[13] to rationalize NMR and dynamic light scattering measurements performed on aqueous solutions of hydrophobically end-capped water-soluble polymers. This model has been developped by Ngai and coworkers[27,28] and assumes a single fast dynamical relaxation in the system. The slow relaxation arises then from the dynamical coupling of the elementary steps through topological and excluded volume interactions. The coupling strength is characterized by a phenomenological coupling parameter $n(C)$ which varies between 0 (no coupling) and 1 and is expected to increase with concentration. At short times, coupling effects do not influence the dynamics and the time correlation function of the scattered field is a single exponential. On larger time scales, coupling effects are responsible for a stretched exponential behavior:

$$\begin{aligned} g^{(1)}(C,q,t) &= \exp[-t/\tau_f(C,q)] \qquad \omega_c t < 1 \\ &= \exp[-(t/\tau_\alpha(C,q))^\alpha] \qquad \omega_c t > 1 \end{aligned} \tag{9}$$

where

$$\tau_\alpha(C,q) = [\alpha\omega_c^{\,1-\alpha}\,\tau_f(C,q)]^{1/\alpha} \tag{10}$$

The exponent α is related to the coupling strength, $\alpha(C) = 1 - n(C)$, and ω_c^{-1} is the characteristic time beyond which coupling effects come into play. Equation 10 links the C and q dependences of the slow relaxation time to those of the fast relaxation time by means of the coupling parameter $n(C)$ (or, equivalently, the exponent α). In particular, at fixed polymer concentration, if the fast relaxation process is diffusive, i.e. $\tau_f \sim q^{-2}$, then one should obtain $\tau_s \sim q^{-2/\alpha}$. Applying this description to our system, one would identify the fast relaxation mechanism as the cooperative diffusion in the semidilute solution. However, the q dependence of our slow relaxation time does not show any systematic influence of the polymer concentration and, within the coupling model, would yield $n(C) \simeq 1/3$ independently of the concentration. This would appear very surprising since these experiments cover a polymer concentration range where the transition between the dilute and semidilute regime can be observed and where one would expect a large increase of coupling effects.

In fact, in the semidilute regime, the entangled chains form a transient network that is deformed when fluctuations of polymer concentration relax cooperatively.[15−19] This network deformation is responsible for a local stress fluctuation that relaxes subsequently on a much longer time scale. The amplitude of this viscoelastic relaxation depends on the ratio of the elastic modulus of the entanglement network to the osmotic modulus of the solution and it is best observed in semidilute Θ solutions.[10]

In associating polymer solutions, the zero shear viscosity η_o is considerably enhanced in comparison with that of equivalent not hydrophobically modified polymer solutions. This enhancement might be related to an increase in both the entanglement network modulus (through the physical associations) and in the longest relaxation time (through mechanisms like sticky reptation[33]). Thus a viscoelastic relaxation might well be expected in these systems. However, the detailed derivation of this model[17] shows no q dependence for the relative amplitude of the slow viscoelastic relaxation, contrary to our experimental results (Figure 4) showing that this relative amplitude increases as the scattering wavevector decreases. In fact, our analysis in the previous section shows that the slow relaxation is associated with the q dependent part of the scattering intensity. It can be noticed that the above mentioned models[15−19,27,28] consider homogeneous solutions for length scales above the semidilute screening length ξ and they leave no place for a q dependence of the scattering intensity in the q range investigated by light scattering experiments.

Such large scale fluctuations of polymer concentration are very easily included in a picture where the slow relaxation is considered to be due to multichain domains that are diffusing in the solution. Such a picture has proved to be useful for the understanding of scattering experiments on polyelectrolyte solutions.[12] In that case, the q dependence of the slow relaxation rate can usually be described as

$$\Gamma_s(q) \equiv \tau_s^{-1}(q) = D_o q^2(1 + A(qR_{app,d})^2) \qquad qR_{app,d} < 1 \tag{11}$$

where D_o is a diffusion coefficient in the vanishing q limit, $R_{app,d}$ is an apparent radius of gyration for the domains obtained from the dynamic experiment, and A is a constant dependent on their structure and polydispersity.[34] Similarly, the scattering intensity can be analyzed as

$$I_s(q) = I_s(0)\left(1 - \frac{1}{3}(qR_{app,s})^2\right) \qquad qR_{app,s} < 1 \tag{12}$$

where $I_s(0)$ is the scattering intensity at zero angle and $R_{app,s}$ is an apparent radius of gyration for the domains derived from the static experiment. Both $R_{app,d}$ and $R_{app,s}$ are apparent lengths since they are not obtained through an extrapolation to zero concentration of the domains. Equation 10 was first derived by Burchard and co-workers in the case of dilute (isolated) polymers with various architectures and polydispersities. When applied to the analysis of domains in polyelectrolyte solutions[12] eqs 11 and 12 yield $R_{app,d}$ and $R_{app,s}$ values within the same order of magnitude.

While the presence of large aggregates seems very likely in solutions where associations through hydrophobic interactions play an important role, the q dependences of the characteristic time and of the scattering intensity associated with our slow relaxation process are markedly different from those in eqs 11 and 12. Pursuing further the idea of domains the $I_s \sim q^{-x}$ and $\tau_s \sim q^{-3}$ behaviors are more consistent with an intermediate scattering regime and the probing of internal modes dynamics. A similar behavior for τ_s has been reported previously for associating polymer solutions in the dilute[31] and semidilute[14] regimes. In ref 14, it was also explicitly stated that the Guinier regime was not observed for the scattering intensity attributed to the presence of aggregates, although no analysis in terms of power law was given. The basic idea remains the same here and means that the slowly fluctuating

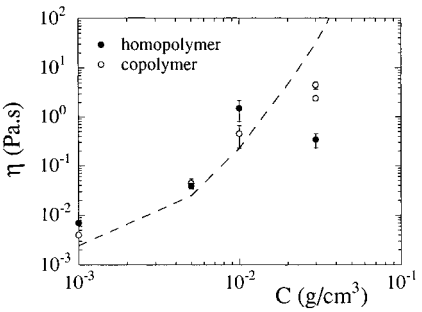

Figure 11. Influence of polymer concentration on the effective viscosity calculated from eq 13 in the text. The dashed line corresponds to values of the zero-shear viscosity of homopolymer solutions interpolated from data in ref 37.

intensity could originate from a texture whose characteristic length L would be much larger than the largest q^{-1} value explored in the experiments, i.e. much larger than 2000 Å. In analogy with dilute solutions of long polymers,[25,26] we would then write

$$\tau_s^{-1} = B\frac{k_B T}{\eta}q^3 \qquad (13)$$

where η is a viscosity and B is a numerical constant. For dilute polymer solutions, η would be the viscosity of the solvent and B would be in the range 0.04−0.08 depending on the quality of the solvent and the method used to calculate it.[26] Now we can argue that if we are dealing with very large objects immersed in a semidilute solution and if we are probing fluctuations with wavelengths much larger than the blob size, i.e. $\xi \ll q^{-1} \ll L$, the viscosity η in eq 13 should be much larger than the solvent viscosity and should tend to the macroscopic viscosity for q^{-1} values much larger than the tube diameter a defined by the entanglements.[35,36] Figure 11 shows η values calculated from the experimental τ_s-(q) values with the use of eq 13 while assuming arbitrarily $B = (6\pi)^{-1}$. The dashed line corresponds to zero-shear viscosity values interpolated from data measured by Kulicke et al.[37] for aqueous polyacrylamide solutions with varying molecular weights and concentrations. The interpolated values have been chosen to match approximately the zero-shear viscosity (29 Pa·s) measured for our polymer N ($M_w = 4.9 \times 10^6$) at $C =$ 0.03 g/cm^3 and correspond to $M_\eta = 3.4 \times 10^6$ for Kulicke et al. This figure calls for a number of comments.

There are several arbitrary constants hidden behind the rather good agreement, at least for $C \leq 0.01$ g/cm^3, between the effective viscosity calculated from eq 13 and the zero-shear viscosity. Among those are the numerical constant B in eq 13 and the numerical factor introduced by our choice for the determination of τ_s (see Experimental Part). Moreover, our samples do not necessarily have the same molecular weight distribution as those investigated by Kulicke et al.[37] Such differences could be expected to show up increasingly as the polymer concentration decreases.

The qualitatively similar variation of the two viscosities for concentrations smaller than 0.01 g/cm^3 appears nevertheless rather striking and suggests that the characteristic time of the slow relaxation is in some way linked to the macroscopic viscosity of the *underlying* semidilute solution. Here we have to emphasize that, due to the hydrophobic associations, the macroscopic viscosity of the copolymer solutions is higher than that of the homopolymer solutions but that the texture seems to probe the solution viscosity of an equivalent homopolymer with the same molecular weight. This link would explain why the characteristic times τ_s are very similar in homopolymer N ($M_w = 4.9 \times 10^6$) and copolymer J ($M_w = 4.0 \times 10^6$) solutions with a trend to larger times for homopolymer N as the concentration increases. Indeed, data from Kulicke et al. show that the molecular weight dependence of the zero-shear viscosity becomes increasingly important for larger concentrations in this concentration range. At $C = 0.03$ g/cm^3, this prevents eventually the measurement of τ_s in homopolymer N solutions while it is still possible for copolymer J solutions. On the other hand, homopolymer D ($M_w = 1.7 \times 10^6$) solutions proved relatively easy to characterize and the estimated effective viscosity is way below that of copolymer J at the same concentration (Figure 11).

Aging effects on the characteristic times τ_s could be understood as well if τ_s is linked to the macroscopic viscosity. Polyacrylamide solutions are known to display a so-called solution viscosity instability,[37] which appears as a decrease in time of the intrinsic viscosity and of the radius of gyration of the chains in dilute solution. Light scattering investigations have shown that the molecular weight remains unchanged and that no degradation occurs. Thus, the mechanism for this solution instability has been assumed to be a conformational change of the coils with the participation of hydrogen bonds.[37] For molecular weights in the range of our study, i.e. intrinsic viscosity $[\eta] \simeq 1150$ cm^3/g, the decrease in that parameter is by a factor of about 0.8 after 30 days.[37] Now it has been also shown that zero-shear viscosity data for polyacrylamide aqueous solutions collapse on a single curve if plotted versus $C[\eta]$. In the range reached in our study for this parameter, i.e. $1 < C[\eta] < 35$, the variation of η_o vs $C[\eta]$ is very steep and can be approximated as a power law with exponent 5.2 when $C[\eta] > 10$.[37] Thus, in that range, a decrease of $[\eta]$ by a factor 0.8 should result in a decrease of the zero-shear viscosity by a factor close to 3 if the aging effects take place as in the dilute solution. This order of magnitude compares fairly well with the corresponding decrease observed for τ_s in time. These aging effects should then be taken into account when trying to find an empirical value for the constant B (eq 13) that would match the effective viscosity and the macroscopic viscosity.

It is, however, necessary to remark on some intriguing points in the above analysis. As said earlier, we would expect to probe a macroscopic viscosity for internal relaxation modes with wavelengths much larger than the tube diameter. However, the tube diameter a is estimated to be at least 1 order of magnitude larger than the blob size,[36,38,39] so that while in our experiments, at least for $C \geq 0.01$ g/cm^3, the condition $q\xi \ll 1$ is fulfilled, the condition $qa \ll 1$ is certainly not for any investigated concentration. At most we have $qa \leq 1$ for $C = 0.03$ g/cm^3. Moreover, the similar behavior of the two viscosities extends down to $C = 10^{-3}$ g/cm^3, which is believed to be below the overlap concentration of the chains or at least below the entangled regime concentration[36] since the macroscopic viscosity at that concentration would be only 2 or 3 times that of the solvent.[37] Should the parallel behavior of the effective viscosity and of the macroscopic viscosity not be fortuitous, this would probably mean that the texture is very "hairy" and that its dynamics is affected by long dangling chains, whose dragging along in the surrounding solution slows down the relaxation of the concentration

fluctuations. This would be a viscoelastic process with a coupling between stress and fluctuations of concentration that could be analyzed along the lines developed by Semenov but allowing for a texture in the solution on length scales much larger than ξ. In principle, a hint for the structure of the texture could be given by the intensity $I_s(q)$ associated with the slow fluctuations, but size polydispersity could affect the values of the exponents found in the intermediate scattering regime.[40]

Coming to that point, we arrive at the conclusion that in the q range investigated by small angle neutron and light scattering experiments, the main significant difference between homopolymer and copolymer solutions is related to $I_s(q)$ and thus it is tempting to link it to the difference in zero-shear viscosities of the solutions. The influence of concentration heterogeneities on solution viscosity has already been examined earlier for polyacrylamide solutions.

Medjahdi et al.[41] have reported detailed light scattering results obtained for polyacrylamide solutions in the dilute and moderately concentrated regimes. They have observed in the small q range an excess of scattering intensity appearing around the overlap concentration and increasing with polymer concentration. This excess of scattering intensity was responsible for a deviation from the Lorentzian intensity shape expected for a semidilute solution and was interpreted on the basis of macromolecular association into aggregates or heterogeneities. They measured in parallel the viscosity of a solution with $C = 0.01$ g/cm^3 and high molecular weight ($M_w = 7 \times 10^6$) and found no evolution in time for both the q dependence of light scattering intensity and the viscosity. They concluded that these heterogeneities "cannot be responsible for viscosity loss reported by some authors".

On the other hand, Kulicke et al. observed that in a plot of the zero-shear viscosity η_o as a function of molecular weight, two distinct regimes could be found with different power law behaviors. They found that the molecular weight $M_\eta \sim 4 \times 10^5$ determining the transition was independent of concentration and nature of the solvent and that the slopes characterizing the molecular weight dependence were significantly different from the values expected from the reptation model. They remarked also that the best data correlation for different molecular weights and concentrations was obtained from a plot of η_o vs $C[\eta]$ and concluded that this viscosity behavior may be understood on the basis of a suspension model and that the entanglement behavior does not seem to control predominantly the viscosity dependence.

Our results in Figure 9 support the finding by Medjahdi et al. that in the semidilute regime, the static scattering intensity in the q range investigated by light scattering is not sensitive to aging. Aging effects are best seen by light scattering in the dilute regime as a decrease of the dimensions of the coils as reported by Kulicke et al.

The question whether the texture has a large effect on the zero-shear viscosity for homopolymer solutions is not entirely clear. On the other hand, for copolymer solutions there are some arguments for such an effect:

(i) The level of $I_s(q)$ relative to $I_f(q)$ suggests that the texture is more important in the copolymer solutions.

(ii) The relative values of the exponents characterizing the power decay of $I_s(q)$ with q would indicate a less compact structure for the texture in the copolymer solution if size polydispersity is not important or is comparable in homopolymer and copolymer solutions.

(iii) Previous rheological measurements on these systems suggested a loose transient network for the structure of the associating domains. Such a structure was found to be easily disrupted by shear flow and to need a very long time (up to several hours) to restore.

Thus it seems natural to identify that loosely connected transient network with the texture observed by light scattering since the latter is characterized by very large length scales and very slow dynamics that suggest a strong viscoelastic coupling with the surrounding solution. On the other hand, in homopolymer solutions, the smallest importance of the texture and its more compact structure (although still with large length scales) might be associated with a texture well below its gel point, i.e. a nonconnecting texture whose influence on the rheological properties would be less critical and might be interpreted by a suspension model, as suggested by Kulicke et al.

V. Conclusions

We have shown that the light intensity scattered from polyacrylamide and hydrophobically modified polyacrylamide solutions can be split into two contributions with very different relaxation times.

The fast mode, characterized by a q independent scattering intensity, corresponds to the contribution of an ideal semidilute solution and the associated fluctuations of concentration relax by the usual cooperative diffusion mechanism of blobs with size ξ.

The slowly fluctuating intensity is responsible for the strong q dependence of the total scattering intensity. It is associated with a texture with characteristic lengths that are too large to be measured in the q range explored in the light scattering experiment. The associated relaxation times vary with the scattering wavevector as a power law with an exponent of about -3. When the polymer concentration is varied, the effective viscosity calculated from the slow relaxation times seems to follow the macroscopic zero-shear viscosity of an equivalent homopolymer solution with about the same molecular weight and concentration over the whole concentration range investigated here.

This suggests that the texture experiences a viscoelastic coupling with the surrounding solution. At present there is no theoretical model available for such an effect. A suitable candidate could be the model developped by Semenov[17] in which the constraint of a solution homogeneous on length scales larger than ξ would be removed.

The coupling between the texture and the surrounding solution can consistently explain aging effects on the slow characteristic times by the solution instability mechanism proposed by Kulicke et al.[37]

The main difference between homopolymer and copolymer solutions lies in their texture, which seems more important and less compact in the latter and could play the role of the loose transient connecting network inferred from previous rheological measurements. In homopolymer solutions, the less important and more compact texture would have a more limited influence on the rheological properties. It would be interesting to investigate in more detail the role of hydrogen bonding in these solutions along the same lines as Sun and King.[14]

Acknowledgment. It is a pleasure to thank S. J. Candau for having initiated the work and for his

continuous interest and support during its progress. A very special thank you is addressed to M. Delsanti for extensive discussions that brought us many clarifications about slow mode dynamics in polymer and colloid systems. We are grateful to J. Selb and F. Candau for careful reading of the manuscript and for kind assistance during the synthesis of the samples in their laboratory. This work has been supported by a PIRMAT joint program.

References and Notes

(1) Hill, A.; Candau, F.; Selb, J. *Prog. Colloid Polym. Sci.* **1991**, *84*, 61.
(2) Biggs, S.; Hill, A.; Selb, J.; Candau, F. *J. Phys. Chem.* **1992**, *96*, 1505.
(3) Hill, A.; Candau, F.; Selb, J. *Macromolecules* **1993**, *26*, 4521.
(4) Valint, P. L.; Bock, J.; Schulz, N. D. *Polym. Mater. Sci. Eng.* **1987**, *57*, 482.
(5) Klucker, R.; Candau, F.; Schosseler, F. *Macromolecules* **1995**, *28*, 6416.
(6) Klucker, R.; Schosseler, F. *Macromolecules*, in press.
(7) de Gennes, P. G. *Scaling Concepts in Polymer Physics*; Cornell University Press: Ithaca, NY, 1979.
(8) Delsanti, M.; Munch, J. P. *J. Phys. II Fr.* **1994**, *4*, 265.
(9) Mathiez, P.; Mouttet, C.; Weisbuch, G. *J. Phys. Orsay* **1980**, *41*, 519.
(10) Adam, M.; Delsanti, M. *Macromolecules* **1985**, *18*, 1760.
(11) Drifford, M.; Dalbiez, J. P. *Biopolymers* **1985**, *24*, 1501.
(12) Sedlak, M.; Amis, E. J. *J. Chem. Phys.* **1992**, *96*, 817.
(13) Nyström, B.; Walderhaug, H.; Hansen, F. K. *J. Phys. Chem.* **1993**, *97*, 7743.
(14) Sun, T.; King, H. E. *Macromolecules* **1996**, *29*, 3175.
(15) Brochard, F.; de Gennes, P. G. *Macromolecules* **1985**, *10*, 121.
(16) Brochard, F. *J. Phys. Orsay* **1984**, *44*, 39.
(17) Semenov, A. N. *Physica A* **1990**, *166*, 263.
(18) Wang, C. H. *Macromolecules* **1992**, *25*, 1524.
(19) Doi, M.; Onuki, A. *J. Phys. II Fr.* **1992**, *2*, 1631.
(20) Berne, B. J.; Pecora R. *Dynamic Light Scattering with Applications to Chemistry, Biology and Physics*; Wiley-Interscience: New York, 1976.
(21) Joosten, J. G. H.; McCarthy, J. L.; Pusey, P. N. *Macromolecules* **1991**, *24*, 6690.
(22) Moussaid, A.; Candau, S. J.; Joosten, J. G. H. *Macromolecules* **1994**, *27*, 2102.
(23) Skouri, R.; Munch, J. P.; Schosseler, F.; Candau, S. J. *Europhys. Lett.* **1993**, *23*, 635.
(24) Provencher, S. W. *Comput. Phys. Commun.* **1982**, *27*, 229.
(25) Dubois-Violette, E.; de Gennes, P. G. *Physics* **1967**, *3*, 181.
(26) Akcasu, A. Z.; Benmouna, M.; Han, C. C. *Polymer* **1980**, *21*, 866.
(27) Ngai, K. L.; Rendell, R. W.; Rajagopal, A. K.; Teitler, S. *Annu. N.Y. Acad. Sci.* **1985**, *484*, 150.
(28) Ngai, K. L.; Rajagopal, A. K.; Teitler, S. *J. Chem. Phys.* **1988**, *88*, 5086.
(29) Stepanek, P.; Lodge, T. P. *Macromolecules* **1996**, *29*, 1244.
(30) Zhou, Z.; Chu, B.; Peiffer, D. G. *Macromolecules* **1993**, *26*, 1876.
(31) Raspaud, E.; Lairez, D.; Adam, M.; Carton, J. P. *Macromolecules* **1994**, *27*, 2956.
(32) Zhang, Y.; Wu, C.; Fang, Q.; Zhang, Y-X. *Macromolecules* **1996**, *29*, 2494.
(33) Leibler, L.; Rubinstein, M.; Colby, R. H. *Macromolecules* **1991**, *24*, 4701.
(34) Burchard, W.; Schmidt, M.; Stockmayer, W. H. *Macromolecules* **1980**, *13*, 1265.
(35) de Gennes, P. G. *J. Chem. Phys.* **1971**, *55*, 572.
(36) Doi, M.; Edwards, S. F. *The Theory of Polymer Dynamics*; Oxford University Press: Oxford, U.K., 1987.
(37) Kulicke, W. M.; Kniewske, R.; Klein, *J. Prog. Polym. Sci.* **1982**, *8*, 373.
(38) Colby, R. H.; Rubinstein, M. *Macromolecules* **1990**, *23*, 2753.
(39) Raspaud, E.; Lairez, D.; Adam, M. *Macromolecules* **1995**, *28*, 927.
(40) Martin, J. E.; Ackerson, B. J. *Phys. Rev. A* **1985**, *31*, 1180.
(41) Medjahdi, G.; Sarazin, D.; François, J. *Eur. Polym. J.* **1990**, *26*, 823.

MA961710L